J Appl Electrochem (2011) 41:1233–1243
DOI 10.1007/s10800-011-0287-y

ORIGINAL PAPER

Evaluation of iodide and titanium halide redox couple combinations for common electrolyte redox flow cell systems

Maria Skyllas-Kazacos · Nicholas Milne

Received: 25 October 2010 / Accepted: 10 March 2011 / Published online: 20 March 2011

Abstract The electrochemical behaviour of a range of halide and titanium halide redox couple combinations has been evaluated for potential application in redox flow cells employing common elements in both half-cells. Cyclic voltammetry and cell cycling measurements were employed to establish the reversibility of the redox couples and the expected cell voltage and performance in a redox flow cell. An all iodine cell was found to be impractical due to the formation of an insoluble iodine deposit in the cell that caused cell blockage. A titanium polyhalide cell that uses a solution of $TiCl_4$ in HBr/HCl supporting electrolyte in both half-cells was, however, shown to produce an open circuit voltage of 0.9 V and high coulombic efficiencies. Although the voltage efficiency of the cell was low, improvements in cell design may reduce ohmic losses allowing much higher energy efficiencies to be achieved. This cell is equivalent to the vanadium bromide cell that employs a vanadium bromide solution in both half-cells. The lower price of titanium, however, opens the possibility of a significant cost benefit for the titanium polyhalide redox flow cell.

Keywords Redox flow cells · Redox couples · Energy storage · Electrolytes

M. Skyllas-Kazacos (✉)
School of Chemical Engineering, The University of New South Wales, Sydney, NSW 2052, Australia
e-mail: M.Kazacos@unsw.edu.au

Present Address:
N. Milne
Institute for Sustainability and Innovation, Victoria University, P.O. Box 14428, Melbourne, VIC 8001, Australia

1 Introduction

There are many electrochemical couples that have been studied and patented as redox flow cell combinations, however, only the all-vanadium redox flow battery [1–17] is approaching commercial reality in stationary applications. The all-vanadium redox flow battery (VFB) uses the aqueous couples:

$$V^{3+} + e \Leftrightarrow V^{2+}$$

$$VO_2^+ + 2H^+ + e \Leftrightarrow VO^{2+} + H_2O$$

The use of vanadium in both half-cells provides an important benefit over most other chemistries proposed to date, in that any mixing of the two half-cells (a common occurrence due to the poor selectivity of most membranes) does not pose a serious problem to the operation and cycle life of the battery. The main disadvantage of the VFB, however, is its relatively low energy density that comes largely from the low solubilities of the V(V) species at elevated temperatures and the V(II), V(III), and V(IV) species at low temperatures. This is coupled with the low electron equivalence of the reaction. As a result the energy density of 15–25 Wh/kg has proven too low for mobile applications, although not a barrier to large-scale stationary applications.

The generation two vanadium bromide redox cell (G2 V/Br) [18], on the other hand, offers a much higher energy density due to the higher solubilities of the vanadium ions in HBr compared with H_2SO_4. Like the all-vanadium redox battery, the G2 V/Br uses the same electrolyte in both half-cells, but in this case, the vanadium ions react at the negative electrode while the halide ions react at the positive.

Although both vanadium battery technologies have the advantage of employing the same electrolyte in both

half-cells, thereby overcoming the problem of cross-contamination, the historical instability in vanadium supply and pricing continues to create uncertainty with regard to the on-going economic viability of the vanadium-based redox flow cells. Considerable effort is now underway to identify alternative redox couple candidates that would potentially utilise the same elements in both half-cells, but employ lower cost and widely sourced raw materials.

1.1 Possible cell combinations

The main advantage of the vanadium redox flow cell chemistries compared to all other chemistries is the use of the same elements in both half-cells that overcomes the problem of cross-contamination. Not only does this allow the solutions to be used indefinitely, without reprocessing, but compared with other chemistries that use different elements in each half-cell, all of the active material is available for reaction. For example, in the case of the original iron-chromium redox flow cell developed by NASA in the 1970s [19, 20], the cross-mixing of the two half-cell electrolytes across the membrane leads to a mixed solution of both iron and chromium in both half-cells with half of each active material unable to participate in each half-cell reaction. This effectively doubles the amount of active material required per unit of stored energy, and thereby doubles the cost of the electrolyte per kWh. The same would apply to any other redox couple chemistry that employs different elements in each half-cell.

When considering possible redox couple combinations therefore, the main criterion used in this study was the possibility of employing the same elements in both half-cells. Cost of the raw materials and cell potential were additional considerations, as was the electrochemical reversibility of the reactions and the likely need for expensive electrode materials or catalysts. Multi-valent elements such as vanadium would be the preferred candidate materials and several such elements can be identified in the periodic table.

A "membrane-less" Pb flow cell that uses the Pb/Pb(II) and Pb(II)/Pb(IV) couple combination has been evaluated by Walsh et al. [21], but the main problem encountered has been the difficulty in controlling the morphology of the solid lead deposits formed at the electrodes during charging. Ideally only soluble species should be formed at both electrodes and electrolyte concentrations of 2 M or more would be required to achieve sufficient energy density for practical application. In addition to vanadium, other elements that exist as soluble species in several oxidation states include Ti, W, Mo, Cr, and iodine.

When considering the use of the same electrolyte in both half-cells, two approaches can be employed:

(i) Type I flow cells: In these cells, ions of the same element in different oxidation states react in each half-cell, as in the case of the all-vanadium redox flow battery that employs the V(II)/V(III) and V(IV)/V(V) couples in the negative and positive half-cells, respectively.
(ii) Type II flow cells: Here the same electrolyte is used in both half-cells, with the cations reacting at one electrode and anions reacting at the other electrode. Examples of this type of flow cell are the Zn/Br [22] and the V/Br [18] flow batteries that utilise the cations and anions at the negative and positive half-cell electrodes, respectively.

Of the aqueous anions, halides such as iodide, bromide, and chloride ions are electroactive and form part of common redox couples that would react in the positive half-cell, while the cation of the halide salt would oxidise and reduce at the negative electrode. Metal salts that could potentially be used as type II flow cell electrolytes would therefore include bromides, chlorides and iodides of titanium, chromium, copper and so on.

In this study, the electrochemical technique of cyclic voltammetry was employed in combination with cell cycling and electrolyte stability studies to evaluate a range of redox couple combinations based on iodine and titanium for use in redox flow cells that have the same solution in both half-cells.

The first possible cell to be considered is the all iodine cell. This has considerable potential in the sense that it uses a single element, making mixing of the two electrolytes of little consequence. The proposed electrode reactions for such a cell would be:

$$IO_3^- + 6\,H^+ + 5\,e \Leftrightarrow {}^1/_2\,I_2 + 3\,H_2O \qquad E^o = 1.2\,V$$

$$I_2 + 2e \Leftrightarrow 2\,I^- \qquad E^o = 0.54\ V$$

The standard potential for this reaction would be approximately 0.66 V in aqueous solutions and although not as high as other combinations, is adequate for the purpose of this study.

The use of the Ti(IV)/Ti(III) couple in combination with polyhalide couples, was also considered for this study. The titanium–bromine cell would give the overall equation:

$$2Ti^{3+} + Br_2 + 2H_2O \Leftrightarrow 4H^+ + 2TiO^{2+} + 2Br^-$$

The standard potential for this reaction is 1.0 V and would be adequate for practical applications [23].

The titanium–iodine cell would involve the overall equation

$$2Ti^{3+} + I_3^- + 2H_2O \Leftrightarrow 4H^+ + 2TiO^{2+} + 3I^-$$

The standard cell potential for this reaction is 0.44 V in aqueous systems and although too low for practical

applications, complexing agents or non-aqueous electrolytes, could potentially be used to shift the reversible potentials of one or both electrode reactions to provide a more useful cell potential.

2 Theoretical background

2.1 Iodine chemistry and electrochemistry

On its own iodine has a solubility of approximately 1.3 mM [24]. However, in combination with soluble halides this can greatly improve. Iodine forms soluble complexes with the halides as I_2X^-. The formation constants for these species can be found in Table 1.

From this information it can be quickly determined that I_3^- is quite stable. Furthermore, iodide salts have relatively high saturation solubilities, e.g., potassium iodide (KI), has a saturation concentration of approximately 8.9 M [24].

The aqueous electrochemical aspects of iodine are fairly well investigated. The results of a study at a platinum electrode by Bard are shown in Table 2 [26].

The kinetics of the electrochemical reactions of iodine are not well understood. However, this is due largely to the effect of absorption of iodine and iodide on the electrode making reproducibility low.

2.2 Titanium chemistry and electrochemistry

Titanium is known in many redox states. It has, however, only been stabilised in four of these states in aqueous solution. The first, titanium metal (Ti^0), does not meet the requirements of a redox flow cell and will not be considered. This leaves the possible soluble species as Ti^{2+}, Ti^{3+}, and TiO^{2+}. These species are related electrochemically by the following two equations [26]:

$$Ti^{3+} + e \Leftrightarrow Ti^{2+} \qquad E^0 = -0.368V$$

$$TiO^{2+} + 2H^+ + e \Leftrightarrow Ti^{3+} + H_2O \qquad E^0 = 0.1V$$

However, titanium species in aqueous solution are notoriously difficult to maintain. In the case of Ti^{2+}, this is due to the reaction with H^+ liberating H_2 and oxidising Ti^{2+} to Ti^{3+}. This essentially means that the use of the Ti^{3+}/Ti^{2+} couple, is limited to electrolytes where the kinetics of the reaction are slow.

TiO^{2+} species are also known to undergo hydrolysis in water. It is believed that in water over a fairly wide pH range the dominant complex species is $[Ti(OH)_4(H_2O)_2]$ that easily rearranges to $TiO_2{\cdot}4H_2O$ [27]. Complexation, has been proposed to minimise, or preferably eliminate the formation of this oxide. There are several complexing agents that have been recommended for solubilising Ti(IV) species. In the redox flow cell used by NASA, Ti(IV) was kept stable through the use of its chloride salt and 3 M hydrochloric acid. This was found to give an E^0 of 0.04 V for the Ti(IV)/Ti(III) couple [28]. This combination forms the complex $[TiCl_6]^{2-}$. There is evidence to suggest that a similar system occurs with both bromide and iodide forming $[TiBr_6]^{2-}$ and $[TiI_6]^{2-}$, although the stability of these complexes is little known.

A commonly used family of complexing agents that works well for TiO^{2+} in aqueous solution is the organic hydroxy acids. The main hydroxy acids used are oxalic, tartaric and citric acids. Oxalic acid is believed to form the complex $[TiO(C_2O_4)_2]^{2-}$ in aqueous solution. It appears to also form the complex $[Ti(C_2O_4)_2]^-$ with Ti^{3+} [29]. This gives the electrochemical equation [26]

$$\left[TiO(C_2O_4)_2\right]^{2-} + 2H^+ + e \Leftrightarrow \left[Ti(C_2O_4)_2\right]^- + H_2O$$

In 0.2 M oxalic acid solution, the half wave potential for the reaction is −0.06 V and was found to be reversible at pH less than three.

The use of the citrate ion as a complexing agent yields the species $[TiO(C_6H_7O_7)]^+$ and $[TiO(C_6H_7O_7)_2]$ [30]. The formation constants for these species are 8.13×10^2 and 3.09×10^2, respectively. At this point in time it is unclear what effect the species has on Ti(III), though there have been suggestions that it may cause the formation of insoluble $Ti(OH)_3$ [27]. A polarographic study of the Ti(IV)/Ti(III) couple in 0.2 M citric acid yielded a half wave potential of −0.13 V, which was found to be reversible [29]. However, in a saturate citric acid solution the reaction proved irreversible.

Table 1 Formation constants for some trihalides [25]

Species formed	From species	*K*
$[I_3]^-$	$I_2 + I^-$	3.85×10^2
$[I_2Br]^-$	$I_2 + Br^-$	13.3
$[I_2Cl]^-$	$I_2 + Cl^-$	2
$[Br_3]^-$	$Br_2 + Br^-$	11.3
$[Br_2Cl]^-$	$Br_2 + Cl^-$	1.4

Table 2 Kinetic parameters of I_3^-/I^- on Pt [26]

c_{I^-} (M)	c_{I_2} (M)	i_0 (mA/cm^2)	i_{0a} (mA/cm^2)	i_{0c} (mA/cm^2)
1.00	0.010	29.0	65.6	21.4
0.50	0.010	20.9	41.6	17.8
0.20	0.010	12.4	21.4	6.2
0.05	0.010	4.3	5.5	2.9
0.20	0.050	18.2	25.1	14.1
0.20	0.002	6.8	14.0	5.0

The tartrate ion creates a situation similar to that of the citrate ion in that the two soluble species appear to be $[TiO(C_4H_5O_6)]^+$ and $[TiO(C_4H_5O_6)_2]$ [30]. The formation constants for these species are 3.16×10^2 and 1.32×10^2, respectively. The polarographic study of the system in saturated tartaric acid produced a reversible reaction with half wave potential of −0.18 V [29].

3 Experimental

3.1 Solution preparation

$TiCl_4$ solutions had to be prepared in a specific way to avoid loss of product or hydrolysis. Concentrated acid was first added slowly, in batches to the $TiCl_4$ until the entire solid dissolves. Water was then added to dilute the components to the required concentration.

3.2 Cyclic voltammetry

Cyclic voltammetric experiments were performed using a Princeton Applied Research Model 173 potentiostat, an EG&G PARC Model 175 Universal Programmer and an analogue recorder connected to a three electrode system. For solutions containing HCl or NaOH, the reference electrode used during the project was a saturated calomel electrode (SCE). In solutions containing sulfuric acid, mercury/mercurous sulfate was used as the reference electrode (potential = 0.62 V vs. SHE).

The working electrode was a 0.6 mm diameter graphite rod embedded in epoxy resin and polished to expose a fixed surface area. Between solutions the electrode was regenerated by polishing the exposed surface with P1200 Tufbak Durite T421 sandpaper and rinsing thoroughly with acetone.

The counter electrode was a graphite rod. This was polished using P1200 Tufbak Durite T421 sandpaper and rinsed in acetone before use in any new solution to avoid contamination.

The cyclic voltammograms were obtained over a range of sweep rates and different voltage ranges depending upon the electrolyte and redox couple being studied.

3.3 Cell cycling experiments

3.3.1 Cell preparation

Each half of the flow cell itself was constructed as shown in Fig. 1.

A piece of Nafion 112 membrane was placed between two half-cells and the cell was then bolted together. Each half-cell comprised a piece of carbon-felt (dimensions 5 × 5 cm), contacted against a sheet of glassy carbon as electrode substrate. A sheet of copper was placed on the other side of the glassy carbon as current collector. Once prepared the cell was connected to the pumps and 25 mL reservoirs filled with the required solutions. These were recirculated through the cell for 30 min before cycling.

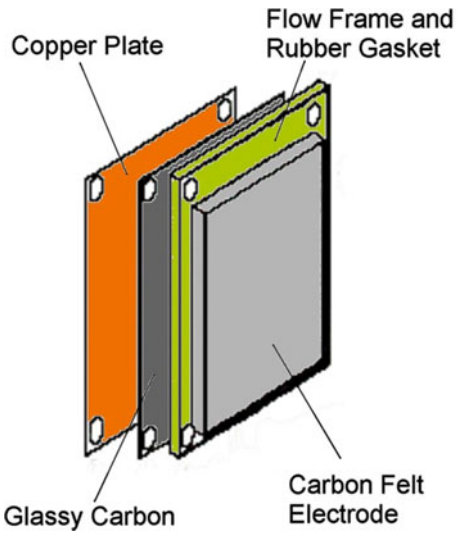

Fig. 1 The construction of half-cell for cell cycling. Two of these are combined and separated by a membrane to form a cell

3.3.2 Operation

The theoretical charge (or discharge) time was calculated using the equation:

$$t = (\mathrm{nFCV})/(\mathrm{I} \times 3600)$$

where t is the time required in hours, n is the number of electron equivalents required per mol of the reacting species, C is its concentration (in mol/L), V is the volume (in L) of the electrolyte in each half-cell and I is the current in amps.

Cells were operated under constant current conditions. The upper voltage limit set for the charge varied depending upon the redox couples used. In general the titanium–iodine system used a maximum voltage of 1 V, the all iodine systems used a maximum of 1.5 V and the titanium–bromine system used a maximum of 1.9 V. In all cases the lower voltage limit set for the discharge cycle was set at 0 V.

3.4 Polarisation studies

Polarisation studies were performed using the same cell described above. The cells were charged to approximately 50% state-of-charge (SOC) as determined from the theoretical charging time and polarisation measurements were

then conducted by applying various charge and discharge currents between 0 and 1 A and recording the cell voltage after approximately 10 s.

4 Results and discussion

4.1 Aqueous iodine studies

4.1.1 General chemistry and electrochemistry

The initial studies of aqueous iodine solutions were performed in HCl in order to establish whether combination with titanium couples could be easily established. From observed precipitation of iodine in the carbon-felt electrode during cell cycling the solubility of the solutions was estimated to be limited to around 2 M I_2 and 5 M KI in 2 M HCl.

Figure 2 shows a typical series of cyclic voltametric scans of the I_2/I^- couple in HCl. Duplicate voltammogram were obtained at each scan rate to verify reproducibility. The main peaks are centred roughly around 0.3 V versus SCE. The appearance of the doublet on the oxidation (forward) sweep is due to the brief formation of the I_3^- complex at the surface of the electrode before I^- is depleted to too large an extent to continue its formation. This is due to the low formation constant of I_3^- in aqueous solution meaning the peaks are not significantly separated and appear as the doublet.

Figure 3 presents the voltammograms obtained in the same solution after the electrode had been soaked for 4 h and then regenerated by polishing the surface with P1200 Tufbak Durite T421 sandpaper, while Fig. 4 shows the voltammograms of nine consecutive scans in the same solution. Both show a decrease in peak currents associated with the I_3^-/I^- couple, with a second set of peaks developing at more anodic potentials. These peaks are believed to represent the IO_3^-/I_2 couple. These results could be due to either the absorption of iodine onto the active sites of the graphite electrode or the formation of a film of iodine on the surface of the electrode during the oxidation of I^- as has previously been documented on platinum and gold [31].

4.1.2 Cell cycling studies

From the electrochemical studies presented above, the possibility of using both the IO_3^-/I_2 and the I_2/I^- couples in a positive and negative half-cells of a redox flow cell, respectively emerged as a possible avenue to explore. A cell was therefore assembled with the same solution of 6 M HCl, 0.5 M I_2 and 1.25 M KI as both the anolyte and the catholyte.

The iodine in this solution was initially fully dissolved but after 35% of the predicted charging time had elapsed, a blockage occurred in the IO_3^-/I_2 half-cell. When the cell was disassembled, the observed site of the blockage in the positive half-cell was recorded as illustrated in Fig. 5.

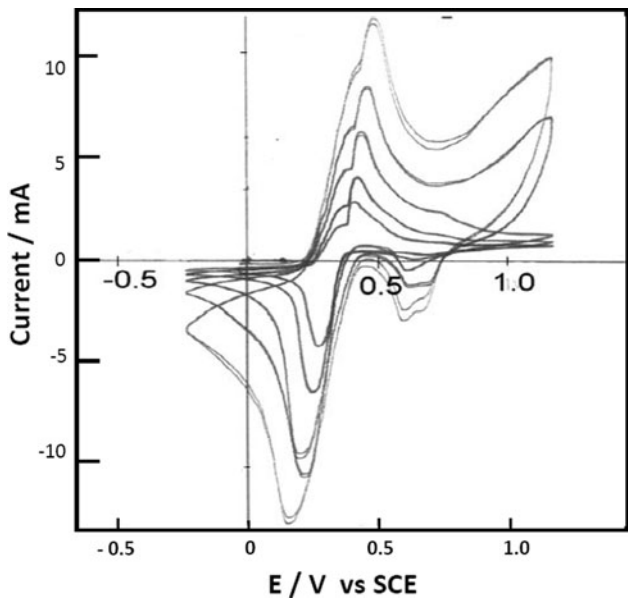

Fig. 2 Typical voltammograms of the I_3^-/I^- couple in HCl using a graphite working electrode and SCE reference at scan rates of 10, 20, 50, 100, and 200 mV/s. Solution composition was 2 M NaI, 0.5 M I_2, and 6 M HCl

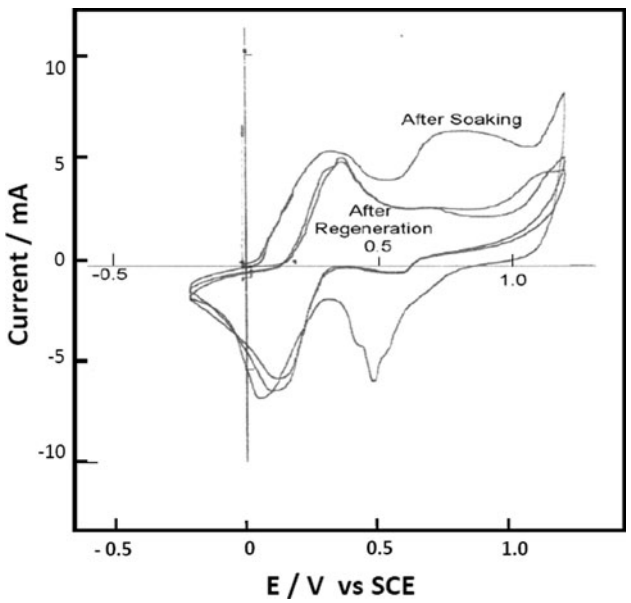

Fig. 3 Voltammogram of graphite electrode in 0.5 M I_2, 2 M NaI, and 6 M HCl obtained at 50 mV/s sweep rate after soaking of electrode for 4 h immediately followed by regeneration of the electrode by polishing

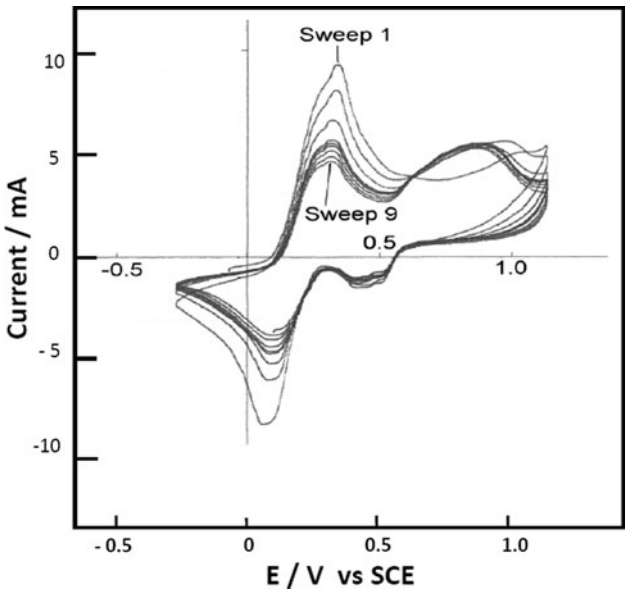

Fig. 4 Voltammograms of graphite electrode in 0.5 M I_2, 2 M NaI, and 6 M HCl, showing nine consecutive scans at a 100 mV/s scan rate with no electrode polishing

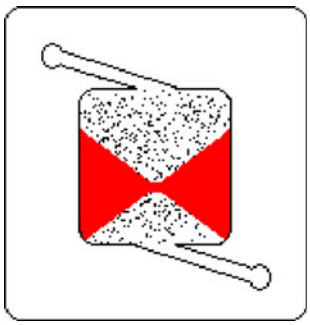

Fig. 5 Diagram indicating the site of blockage (*solid shading*) in the positive electrode chamber during the cycling of a flow cell employing a solution of 0.5 M I_2, 1.25 M KI, and 6 M HCl in both half-cells. The precipitate appears to be I_2 formed during the reaction between I^- and IO_3^-

It was quickly apparent that the blockage had occurred due to the formation of excess I_2 in the solution. This was simply due to the nature of the reaction being studied. In the IO_3^-/I_2 half-cell the electrochemical reaction taking place is:

$$I_2 + 6H_2O \Leftrightarrow 2IO_3^- + 12H^+ + 10e^-$$

Excess iodide is essential in forming the I_3^- complex and therefore keeping I_2 soluble. However, in the presence of iodate, iodide reacts according to the following equation:

$$10I^- + 2IO_3^- + 12H^+ \Leftrightarrow 6I_2 + 6H_2O$$

This means that in the presence of iodate, the concentration of I_2 will increase while that of I^- will decrease, eventually preventing the formation of I_3^- in areas of the cell where I^- levels drop too low and therefore the precipitation of I_2 occurs.

The solubility of iodine has thus appeared as an important consideration when investigating the possible use of iodine in a redox flow cell. This is not just in relation to possible precipitation, but also with regard to the iodine film effect. The use of semi-aqueous iodine systems is considered as a possible solution for future study.

4.2 Aqueous titanium studies

4.2.1 Solution characteristics

The formation of Ti(IV) solutions from $TiCl_4$ in acid halides goes through numerous stages during acid addition. Table 3 depicts the various observations at different volume additions of 48 wt% HBr to 26.72 g (0.14 mol) of $TiCl_4$.

Initial addition of some acid results in yellow solid coated in red solution. After the addition of more acid a large plume of fumes escapes the flask. More red solution is formed as the amount of solid in the flask grows. After 25 mL of HBr is added a red solution with yellow residue remains. After the further addition of HBr the solution remains red but with excess acid, the final appears straw yellow in colour.

The above colour changes occur regardless of the acid used with the exception of the final colour. In HCl this colour is a pale yellow, in HBr a bright yellow and in the presence of the iodide ion a dark orange to red solution is formed. Titanium tetrachloride fumes naturally when exposed to air and forms a pale yellow solid. This is due to the partial hydrolysis of the $TiCl_4$ by moisture in the air, producing HCl [27]. As the solution is already saturated the HCl is released as a vapour, thereby created the fumes seen in the system. Upon the addition of the acid this hydrolysis becomes much more intense resulting in the large production of vapours and the formation of significant amounts of solid. The use of the acid to dissolve the $TiCl_4$ ensures that full hydrolysis of $TiCl_4$ to the solid TiO_2 does not take place. As a result the solid is soluble in excess acid and a solution of known titanium concentration can thus be achieved.

The large ratio of Br^- to Ti(IV) achieved before the final colour change indicates that a large excess of bromine is required to form the halide complex. This suggests that the complex probably includes Br^- ligands. As a result of the colour and the large ratio required $TiBr_4Cl_2^{2-}$ seems to be the most likely species formed.

The formation of the titanium complex with iodide could only be achieved through the use of NaI solution acidified with HCl. This dissolution proceeded similarly to those in HCl and HBr with the exception of the formation

Table 3 Observations during the addition of 8.4 M HBr to 26.72 g $TiCl_4$ slowly with vigorous mixing

Volume HBr added (mL)	Observations	Ratio Br^- to Ti^{IV}
0	Fuming, small amounts of white solid formed	–
<25	Copius fuming. Large amounts of yellow solid formed. Cherry red solution.	–
25	All solid dissolved. No fuming. Cherry red solution.	1.5
70	Orange solution.	4.2
120	Bright yellow solution	7.2
>120	Yellow solution fades.	–

of an apparently white solid in the orange-red solution. This has been attributed to the formation of the salt $Na_2[TiCl_4I_2]$ from the univalent cation as predicted by Nicholls [27].

It appears that pH is the decisive factor when ensuring the solubility of Ti(IV) in aqueous solution. $TiCl_4$ solutions in both HBr and HCl began to form TiO_2 at a pH of 1.1 with significant oxide production at 1.5. As the pH rises the effect of these complexing agents quickly becomes negligible. The formation of TiO_2 and the blockage of the cell as a consequence could therefore becomes a serious possibility in these situations. It should be possible to overcome this problem using as low a pH as is possible in the electrolyte.

4.2.2 *Cyclic voltammetry*

Figure 6 shows a typical scan of the titanium system in HCl. The peaks centred around 0 V versus SCE are believed to represent the Ti(IV)/Ti(III) couple. In a high concentration of hydrochloric acid this is represented by the equation:

$$TiCl_6^{2-} + e^- \Leftrightarrow TiCl_4^- + 2Cl^-$$

where the two species are distinguishable by colour—$TiCl_6^{2-}$ is pale yellow to colourless while $TiCl_4^-$ is deep purple.

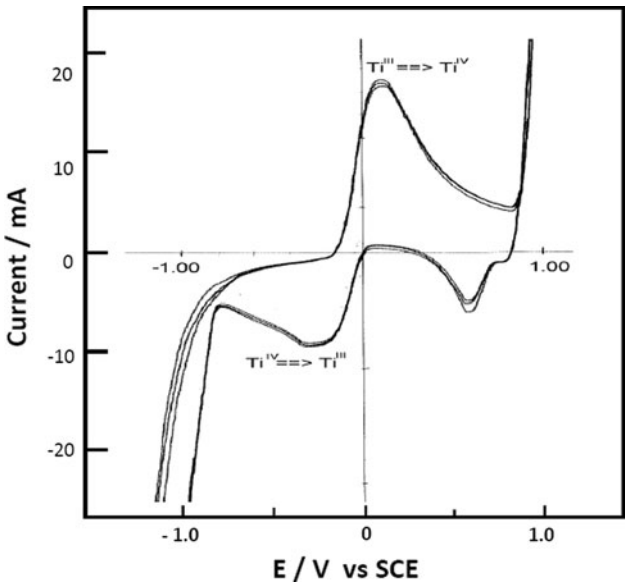

Fig. 6 A typical cyclic voltametric scan of graphite electrode in solution of 0.5 M TiCl3, 6 M HCl at a scan rate of 50 mV/s

The plot of peak current versus the square root of scan rate was linear for both the oxidation and reduction peaks suggesting that both reactions are diffusion controlled. The formal potential calculated for the reaction, 0.06 V, compares well with the value of 0.04 V calculated by Wang [28].

No further peaks are observed at more negative potentials before the region for hydrogen evolution, confirming that Ti(II) species cannot be produced in this solution. This supports the previous results reported by Bard [26] that the Ti(III)/Ti(II) couple is not thermodynamically favoured in aqueous systems. At 0.8 V versus SCE, the onset of chlorine evolution is observed, the chlorine reduction peak appearing at 0.6 V during the reverse cathodic scan

The addition of citric acid to the solution resulted in some distinct changes to the voltammogram as seen in Fig. 7.

Most importantly, the potential for the reduction of Ti(IV) shifted to more negative potentials, while a second Ti(III) oxidation peak appears at −0.2 V. The benefit of this potential shift is important since it means that the lower Ti(IV)/Ti(III) half-cell potential will produce higher overall cell voltage during discharge.

When HCl was replaced by HBr, the typical voltamogram shown in Fig. 9 was obtained. The formal potential for the Ti(IV)/Ti(III) couple was 0.00 V similar to that in the HCl acid system.

Bromine evolution and the corresponding reduction peak is also observed in Fig. 8. The formal potential for the Br_2/Br^- couple was calculated as 1.06 V (SHE), comparing well with the standard potential of 1.1 V reported by Aylward and Findlay [24].

The peak potentials of the Ti(IV)/Ti(III) couple showed negligible change with scan rate and it is therefore considered to be largely reversible. A plot of i_P versus $v^{1/2}$ (see

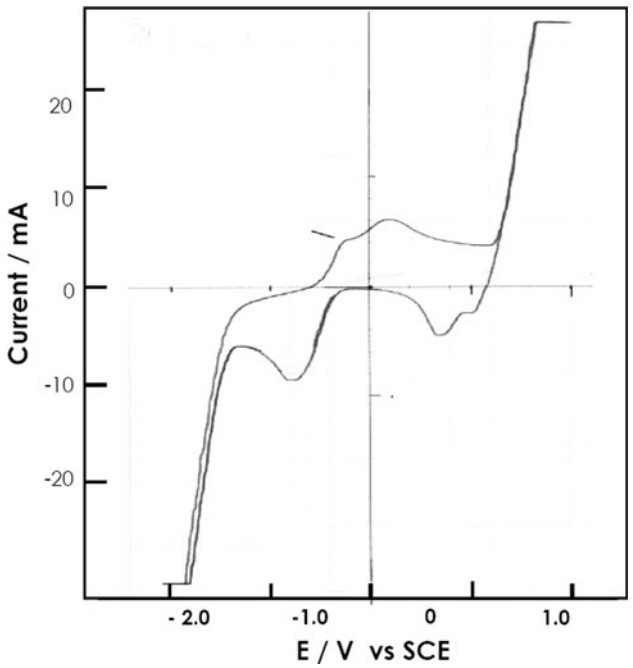

Fig. 7 Typical voltammogram at graphite electrode in solution of 0.5 M $TiCl_3$, 0.25 M citric acid, 0.75 M HCl at a scan rate of 200 mV/s

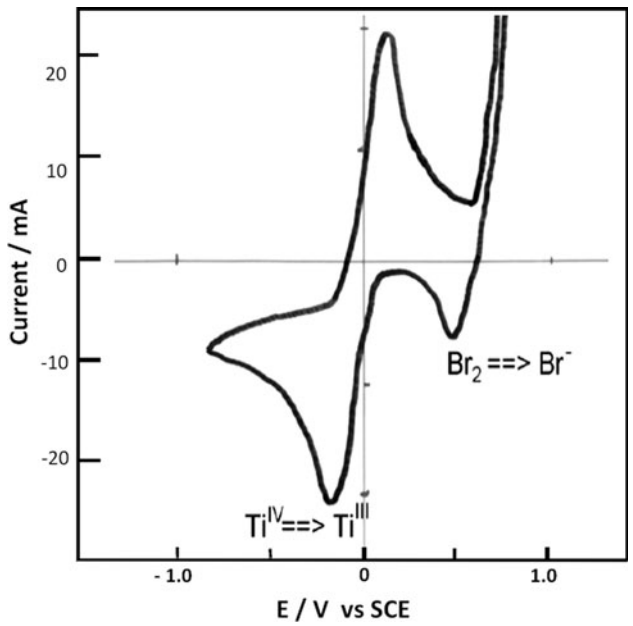

Fig. 8 Typical cyclic voltametric scan of graphite electrode in 2 M $TiCl_4$, 4 M HBr, 3 M HCl at a scan rate of 50 mV/s

Fig. 9) was linear suggesting these reactions are diffusion controlled.

The Br_2/Br^- couple appeared to be shifted slightly in the negative direction. This was confirmed with the formal potential of 0.98 V. The shift is not particularly significant

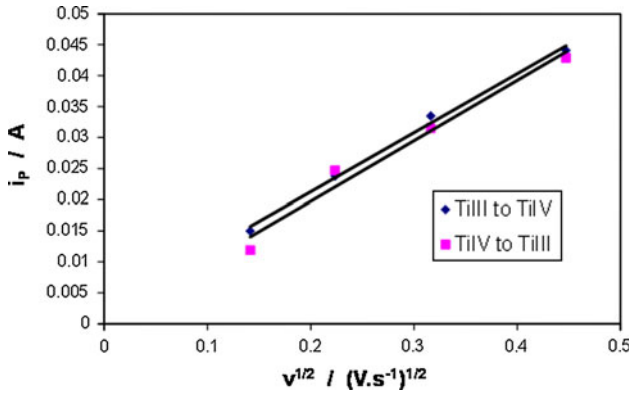

Fig. 9 Plot of peak current versus the square root of scan rate for the Ti(IV)/Ti(III) couple peaks in Fig. 8

but may represent the increasingly important role of the polyhalide species Br_2Cl^-.

4.2.3 Cell cycling studies

In the first cell run the solutions used were $TiCl_4$, HBr, and HCl mixtures for the anolyte and an HCl/NaBr mixture for the catholyte. The expected negative and positive discharge reactions, respectively for the titanium polyhalide cell are:

$$TiBr_2Cl_2^- + 2Cl^- \rightarrow TiBr_4Cl_2^{2-} + e^-$$

$$Br_2 + 2e^- \rightarrow 2Br^-$$

The results of the cell cycling are shown in Fig. 10 for a charging and discharging current of 1 A (40 mA/cm^2). The large voltage difference between the charge and discharge curves shows a high ohmic resistance and overpotential losses. There was also a large amount of solvent transfer in the cell from the catholyte to the anolyte. This eventually resulted in the drying up of the catholyte and the overflow of the anolyte reservoir and is a property strongly undesired in the system. It is believed that the water transfer was due to the higher ionic strength in the anolyte due to the presence of titanium salts and the general higher concentrations for this system. To this extent it was

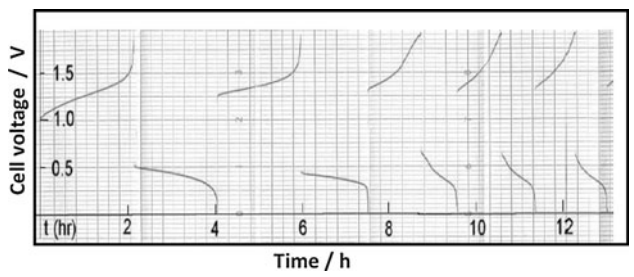

Fig. 10 Charge-discharge profiles for the titanium halide cell employing 2 M $TiCl_4$, 3 M HCl, and 4 M HBr as the anolyte and 4 M HCl and 2 M NaBr for the catholyte

believed that running the same solution as both the anolyte and the catholyte would help to reduce this effect.

As would be expected, the result of the solvent transfer was a blockage of the cell. However, as seen by Fig. 11, when the cell was dismantled, the extent of this blockage was not as significant as expected. The blockage was of an orange solid and was believed to be NaBr and NaCl in the presence of a residual Br_2 solution. It appears that a large majority of the salts present in the catholyte were in fact transferred to the anolyte.

Figure 12 shows a plot of coulombic efficiency versus cycle number. A large decrease in the charge and discharge times was observed during cycling and was probably due to the significant transfer of active material across the membrane. As a result of this transfer the coulombic efficiencies also varied but are in general in the range 80–90%.

As a result of the water transfer a solution of 4 M HBr, 3 M HCl, and 0.56 M $TiCl_4$ was prepared that could be run as both the anolyte and the catholyte. The first charge–discharge cycle gave a coulombic efficiency of 93%. Figure 13 contains the first two full charge discharge profiles for the system.

A plot of the charge and discharge times versus cycle number is provided in Fig. 14. This shows a significantly high coulombic efficiency (97–98%) and no significant decrease in the charge or discharge times as the number of cycles increased. However, this may not hold at higher $TiCl_4$ concentrations as more Br_2 gas will be formed with the greater possibility for escape. In this case some of the active materials may be lost and the coulombic efficiency would drop as a result.

The above cell cycling experiment was performed on the above solution after it had been sitting over a 72 h period. Over this time the solution was not cycled. Before the system was discharged to begin the cell cycling and before the pumps were restarted the open circuit potential was measured to determine the extent of self-discharge. There had been a drop in the cell voltage from around 0.6 to

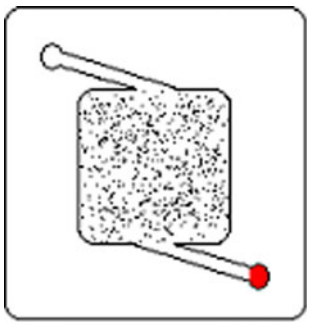

Fig. 11 Diagram showing the location of blockage (*solid shading*) in the positive electrode chamber when using an anolyte of 2 M $TiCl_4$, 3 M HCl, 4 M HBr and a catholyte of 4 M HCl, 2 M NaBr

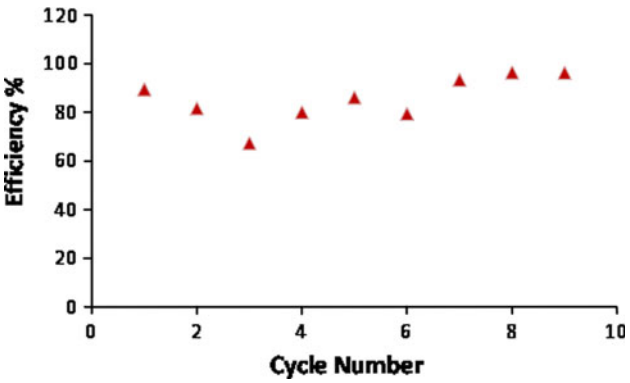

Fig. 12 Plot of coulombic efficiency versus cycle number for the titanium halide cell with anolyte of 2 M $TiCl_4$, 3 M HCl, 4 M HBr and catholyte of 4 M HCl, 2 M NaBr when using a charge and discharge current of 1 A

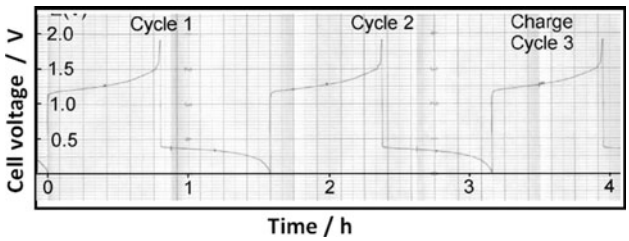

Fig. 13 Charge-discharge profile for the titanium polyhalide cell using 0.5 M $TiCl_4$, 3 M HCl, 4 M HBr as both the catholyte and the anolyte for a charge and discharge current of 1 A (electrode area = 25 cm^2)

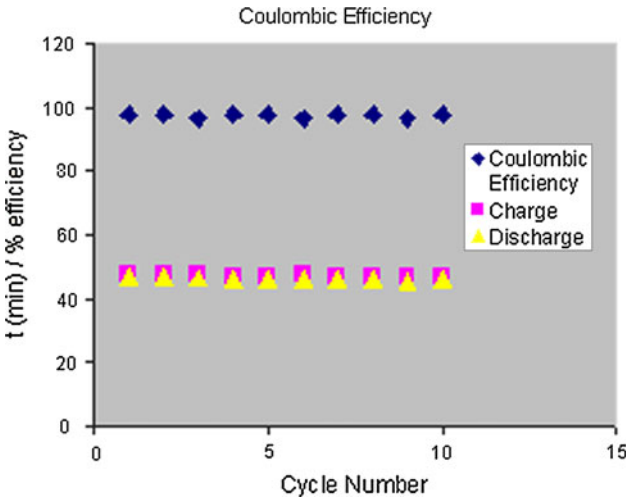

Fig. 14 Plot of charge and discharge time and coulombic efficiency for the titanium polyhalide cell using 0.5 M $TiCl_4$, 3 M HCl, 4 M HBr as both anolyte and catholyte at a charge and discharge current of 1 A

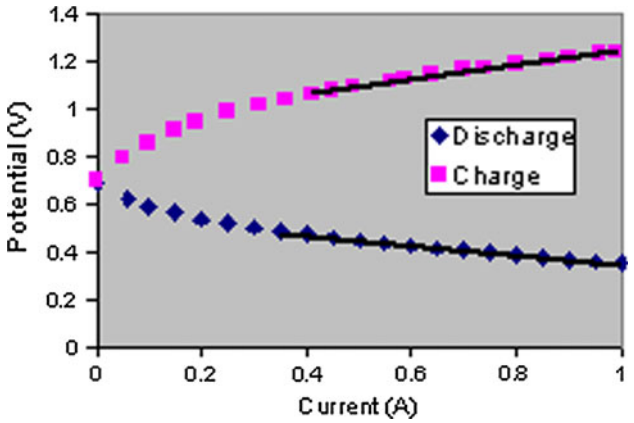

Fig. 15 Polarisation plots for the titanium polyhalide cell at approximately 50% SOC using 0.5 M $TiCl_4$, 3 M HCl, 4 M HBr as both the anolyte and catholyte

0.4 V because of self-discharge of the charged species across the membrane.

The open circuit potential obtained when the cell was fully charged was found to be 0.93 V, this representing the highest open circuit potential obtained in this the study. The cell was then discharged to approximately 50% SOC and the potential at various charge and discharge currents was measured. Figure 15 show the resulting cell polarisation plots obtained.

From the slopes of these plots the cell resistance can be calculated as 7 and 5 Ω cm^2 for the charge and discharge processes, respectively. These values show that the resistance associated with the charging process is much greater than the discharging. The possible reason for this may be the high stability of the Ti(IV) species the greater energy required to break the bonds during the reduction process. Another reason for the higher charging resistance may be the formation of bromine gas during the charging process.

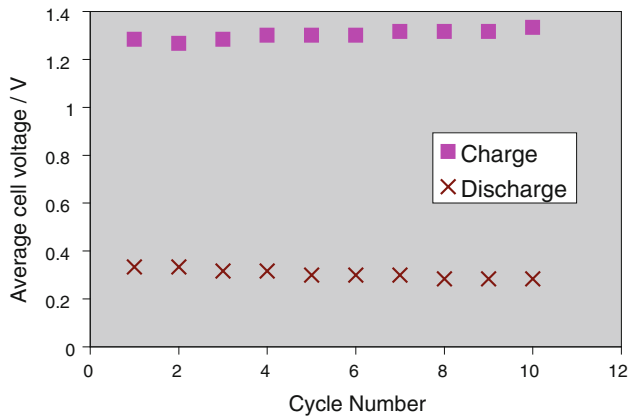

Fig. 16 Plot of average charge and discharge cell voltages versus cycle number for the titanium polyhalide cell using the electrolyte 0.5 M $TiCl_4$, 3 M HCl, 4 M HBr as both anolyte and catholyte

Generally, during charging cycle, a gas, presumably bromine, was observed bubbling out the cell. The presence of these bubbles inside the positive half-cell cell cavity would introduce a significant resistance and as a result, lower voltage efficiencies would be expected.

Figure 16 shows a plot of the median potential value for the cell during both charge and discharge against cycle number. In this case the voltage efficiency appears to be quite low. However, this may be at least partially remedied by the improvement of the cell design to reduce the internal resistances. Some reduction may also be possible in the use of additives in the electrode materials to catalyse the reactions and reduce overvoltage losses.

5 Conclusions

From the results obtained in this study, it appears obvious that the use of iodine in a redox flow cell is limited. The all iodine aqueous redox flow cell evaluated in this study showed solubility problems associated with elemental iodine that makes its use prohibitive. The inherent instability of iodate in HCl and the apparent irreversibility of the IO_3^-/I_2 couple in sulfuric acid also suggests there would be a potential problem in long term applications of such a cell. The use of semi-aqueous systems may have some possible applications in the future if the correct solvent can be found. Further studies with semi-aqueous systems are therefore warranted.

The most promising cell emerging from the study appears to have been the titanium polyhalide cell. Its open circuit voltage of 0.9 V coupled with its high coulombic efficiencies lends itself for further development into its potential use. Although the voltage efficiency of the cell was low, improvements in cell design may reduce ohmic losses allowing much higher energy efficiencies to be achieved. This cell is equivalent to the vanadium bromide cell that employs a vanadium bromide solution in both half-cells. Since titanium has historically shown a much lower price structure compared with vanadium, however, the substitution of vanadium with titanium, opens the possibility of a significant cost benefit for the titanium polyhalide redox flow cell. For example, in August 2010, TiO_2 prices averaged at around USD1/lb (USD0.18 per mol Ti) compared with V_2O_5 prices at around USD6.50/lb (USD1.3 per mol V). This significant difference in vanadium versus titanium prices should more than offset the additional processing costs of the titanium electrolyte, however, considerable work is still needed to fully develop a titanium polyhalide redox flow battery for long cycle life and efficient operation over a range of temperatures and operating conditions.

References

1. Skyllas-Kazacos M, Robins, R (1986) All-vanadium redox battery, US Pat. 4786567
2. Skyllas-Kazacos M, Rychcik M, Robins R, Fane A, Green M (1986) J Electrochem Soc 133:1057
3. Skyllas-Kazacos M, Grossmith F (1987) J Electrochem Soc 134:2950
4. Rychcik M, Skyllas-Kazacos M (1988) J Power Sources 22:59
5. Sum E, Skyllas-Kazacos M (1985) J Power Sources 15:179
6. Sum E, Rychcik M, Skyllas-Kazacos M (1985) J Power Sources 16:85
7. Zhong S, Skyllas-Kazacos M (1992) J Power Sources 39:1
8. Skyllas-Kazaocs M, Rychcik M (1987) J Power Sources 19:45
9. Kazacos M, Cheng M, Skyllas-Kazacos M (1990) J Appl Electrochem 20:463
10. Skyllas-Kazacos M, Kasherman D, Hong R, Kazacos M (1991) J Power Sources 35:399
11. Largent R, Skyllas-Kazacos M, Chieng J (1993) Proceedings IEEE, 23rd photovoltaic specialists conference. Louisville, Kentucky
12. Menictas C, Hong D, Yan Z, Wilson J, Kazacos M, Skyllas-Kazacos M (1994) Proceedings, Electrical Engineering Congress. Sydney, NSW
13. Skyllas-Kazacos M, Menictas C, Kazacos M (1996) J Electrochem Soc 143:L86
14. Skyllas-Kazacos M, Peng C, Cheng M (1999) Electrochem Solid State Lett 2:121
15. Kausar N, Howe R, Skyllas-Kazacos M (2001) J. Appl Electrochem 31:1327
16. Rahman F, Skyllas-Kazacos M (2009) J. Power Sources 189:1212
17. Skyllas-Kazacos M, Kazacos G, Poon G, Verseema H (2010) Int J Energy Res (Energy storage special issue) 34:182
18. Skyllas-Kazacos M (2003) J. Power Sources 24:299
19. Hagedorn N, Thaller L (1980) NASA Report Number: DOE/NASA/1002-80/5, E-383, NASA-TM-81464
20. Giner J, Cahill K (1980) NASA Report Number: DOE/NASA/0794-80/1, NASA-CR-159738
21. Wills R, Collins J, Stratton-Campbell D, Low C, Pletcher D, Walsh F (2010) J Appl Electrochem 40:955
22. Singh P, Jonshagen B (1991) J. Power Sources 35:405
23. Bartolozzi M (1989) J. Power Sources 27:219
24. Aylward G, Findlay T (1998) SI chemical data, 4th edn. Wiley, Australia
25. Mironov V, Lastovkina N (1967) Russ J Phys Chem 8:991
26. Bard A (1973) The encyclopaedia of the electrochemistry of the elements. Marcel Dekker Inc, New York
27. Nicholls D (1974) Complexes and first row transition elements. MacMillan Press, London
28. Wang Y, Lin M, Wan C (1984) J. Power Sources 13:65
29. Pecsok R (1951) J Am Chem Soc 73:1304
30. Zolotukhin V, Gnatyshin O (1973) Russ J Inorg Chem 18:1467
31. Swathirajan S, Bruckenstein S (1980) J Electrochem Soc 112:25